# ON THE INFLUENCE OF MICROSTRUCTURAL FEATURES OF LINEAR FRICTION WELDING AND ELECTRON BEAM ADDITIVE MANUFACTURING TI-6AL-4V ON TENSILE AND FATIGUE MECHANICAL PROPERTIES

Michael Mendoza (ISU)
Faculty: Peter Collins (ISU)
Industrial Mentor: Honeywell

## 35.1 Project Overview and Industrial Relevance

This research provides a study of Linear Friction Welding (LFW) and Electron Beam Additive Manufacturing (EBAM) of the alloy Ti-6Al-4V. Currently these technologies are suitable for many aerospace applications and, in particular for integrated blisks (i.e. aeroengine compressor discs with blades). However, more studies to understand the individual microstructure influence on mechanical properties are required. In this work, dogbone shape specimens were extracted from LFW-Ti-6AL-4V to individually assess the tensile mechanical properties of the Welded Zone (WZ), Thermo-mechanically affected Zone (TMAZ) and the Parent material zone (PM) across the weld line. Beam shape specimens were also extracted from EBAM-Ti-6Al-4V to evaluate the individual microstructure influence on fatigue mechanical properties by a four-point bending test. Finally, COMSOL Multiphysics software was used to predict shape and dimensions of cantilever specimens from EBAM-Ti-6Al-4V to again assess the individual microstructure influence on fatigue mechanical properties, but to a very high cycle's regime ($10^9$ Cycles). For this last section, a commercial ultrasonic welding machine will be adapted to perform the fatigue tests.

The study of Ti-6Al-4V under different manufacturing processes is attracting more interest from industry because of cost reduction and potential improvements in mechanical properties. The main advantage of LFW resides in the fact that for aircraft structural components oversized ingots are machined to get the final component, so a large amount of material is wasted. LFW allows the use of not oversized ingots for welding them together to form the component with less use of initial material.

## 35.2 Previous Work – Literature Review

The study of Ti-6Al-4V under different manufacturing processes is attracting more interest from industry because of cost reduction and potential improvements in mechanical properties. Each manufacturing process (e.g. LFW, EBAM, LENS, Casting, etc.) has its own particularities in terms of thermal or thermomechanical histories that affect local microstructures. However, we will focus on LFW that offers unique thermomechanical conditions and EBAM that provides bigger microstructural features than other AM processes which makes the analysis easier. Linear Friction Welding LFW is a solid-state joining process of two workpieces under compressive forces [35-1] (Fig. 1a). During the process, one workpiece is stationary while the other one is in motion, this friction generates heat that plasticize the contact zone and a final forging pressure is applied to consolidate the joint [35-2]. The current and major use of LFW is for joining of aeroengine compressor discs with blades to form blisks [35-3, 35-4, 35-5, 35-6] (Fig. 1b). However, there is more recent interest for aircraft structural components made of Ti-6Al-4V [35-6]. The main advantage of LFW resides in the fact that for aircraft structural components oversized ingots are machined to get the final component, so a large amount of material is wasted. Smaller workpieces can be joined with LFW to produce a component, so less material is required as an initial step [35-6]. Vairis and Frost [35-7, 35-8] describe the process into four distinct phases. At phase I, the two workpieces are placed into contact under certain pressure. The contact area is augmented with reduction of asperities and heat generation due to solid friction. In phase II, the heat generation is enough to increase the area of contact to a 100% and expulsion of viscous material from the interface (i.e. initial flash formation). In the specific case of Ti-6Al-4V, it is when the interface reaches the β-transus temperature [35-9]. Phase III is the equilibrium phase, here the flash formation is more visible and the axial shortening is present at a constant rate [35-6]. Phase IV is known as deceleration and forging phase where in less than 0.1 s the two workpieces are brought to rest and a final forging pressure is applied to finish the joint. LFW-Ti-6Al-4V can produces three different zones, parent or base material (PM) with a bi-modal microstructure (i.e. primary $\alpha_p$ grains surrounded by a lamellar microstructure of $\alpha$ laths

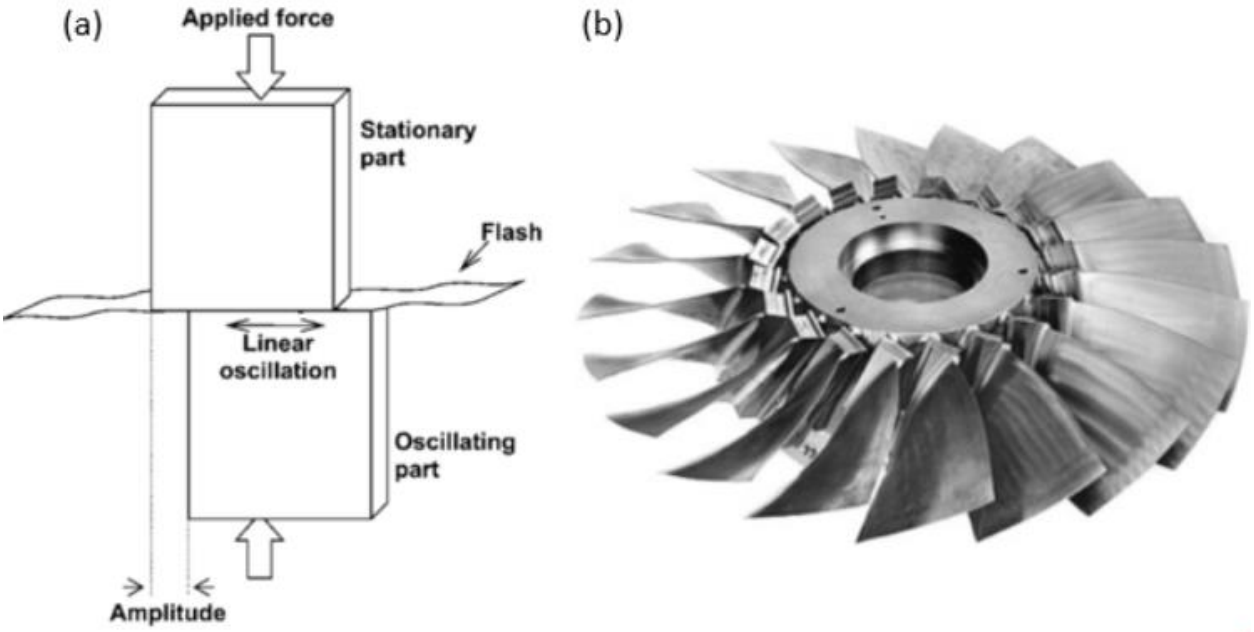


Figure 1.(a) Diagram of Linear Friction Welding process, (b) Integrated blisk (disc and blades) [35-3].

in a β matrix), thermo-mechanically affected zone (TMAZ) with a distorted bi-modal microstructure and a weld zone (WZ) with a refined martensitic α' (needle-like) or a widmanstatten microstructure depending on the cooling rate (Fig. 2).

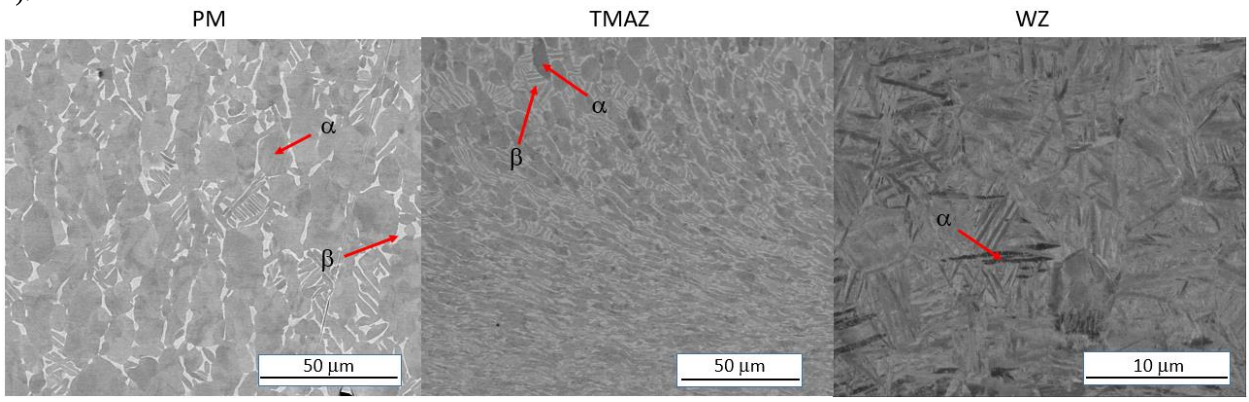


Fig. 2 Microstructure change across a LFW joint.

As mentioned, this research focus into the Ti-6Al-4V alloy and some mechanical properties according to the microstructure as a consequence of the manufacturing process. The conventional approach to evaluate tensile mechanical properties for LFW of Ti-6Al-4V is by consideration of processing parameters as the frequency of oscillation, amplitude, frictional pressure and axial shortening [35-1, 35-6, 35-10, 35-11, 35-12]. However, our approach will be just to evaluate specific tensile properties of given LFW-Ti-6Al-4V microstructures at certain constant processing parameters. To date most of the results for tensile test show failure at the parent material zone (PM) if not interface contaminants are present [35-1, 35-6, 35-10, 35-11, 35-12]. However, Wanjara and Jahazi [35-1] also showed that failure can also occur on the TMAZ due to a low power input that reduce the cooling rate after oscillatory motion, making the alpha laths bigger which in turn makes the TMAZ weaker than PM [35-6]. Our approach is to evaluate the specific tensile properties of the three zones of LFW-Ti-6Al-4V by forcing the tensile samples to fail at the respective zone. Characterization techniques as SEM, EBSD, TEM and PED will help us to determine the reasons of those differences in tensile properties.

Additive manufacturing process (AM), also known as 3D printing is a rapid solidification process that

involves several factors affecting the final microstructure. By definition AM is a process where a local heat source (e.g. laser, electron beam, plasma) melts a source of material (e.g. incoming powder flow, wire, powder bed) on a substrate of similar characteristics of the material [35-13]. The relative motion between the heat source and the substrate allows the melted material deposition to occur layer by layer, always under a computer aid control from a CAD file [35-13] (Fig. 3). This particular way to produce parts offers several advantages as near net-shape components with very low final machining required, complex parts are easy to make with the right CAD file, less waste of material as compared with subtractive manufacturing technologies and new possibilities in terms of microstructure control.

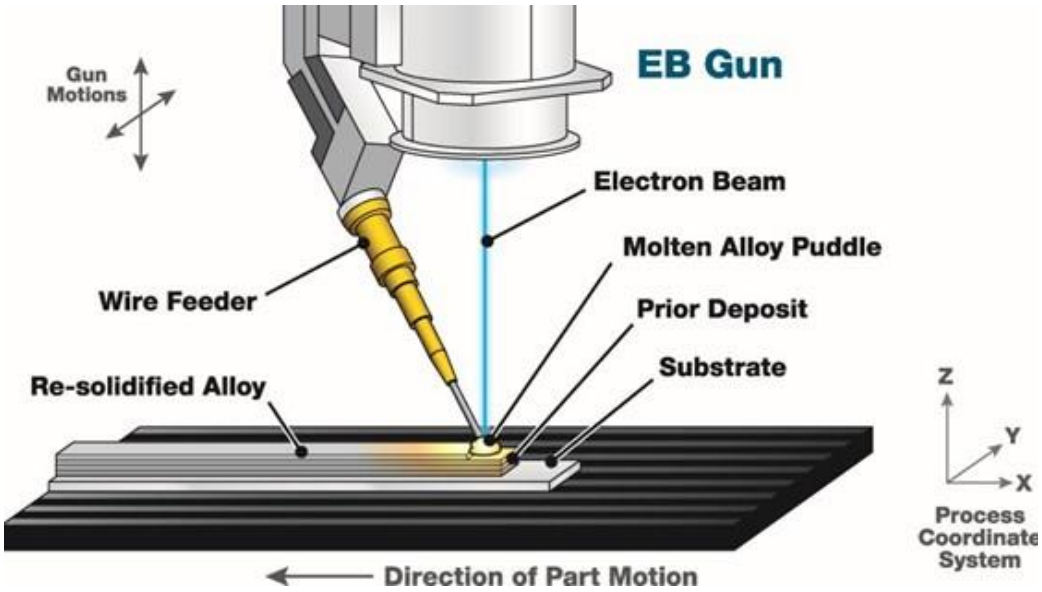


Fig. 3 Schematic EBAM® process [35-14].

In this study, we will focus into the Electron Beam Additive manufacturing technique EBAM® that uses an electron beam as heat source, Ti-6Al-4V wire as feedstock and a vacuum chamber to protect the alloy to react with oxygen. In Fig. 4 characteristic features of EBAM-Ti-6Al-4V are observed in the *z-y* cross-section being *x* the direction of deposition (out of paper). Two distinct zones can be recognize on this picture, zone A comprises vertically elongated prior β grains with very little variation in α lath thickness due to the uniform and strong epitaxial growth from bottom to top [35-15]. On the other hand, Zone B has a pronounced variation in α lath thickness and a more scattered orientation due to the competing growth from the side wall of the molten pool [35-15]. Several tensile tests were already reported on those microstructures to assess their influence on tensile mechanical properties [35-15]. Therefore, the interest of this research is in mechanical properties from a fatigue test on those two type of microstructures. Four-point bending test is selected as a convenient method for fatigue studies due to several reasons (Fig. 5). It typically works with rectangular beams that produce a uniform maximum stress on the surface, depending of the distance between inner rollers [35-16]. Easy sample mounting and dismounting as no special gripping is required. It is also suitable to evaluate specific microstructures from small samples, T. Zhai et al. [35-16] reported specific sample and device dimensions to perform the four-point bending test. The optimum testing geometry to achieve a uniform stress distribution consistent with the calculated value of beam theory, requires a load span/specimen thickness ratio (*t/h*) between 1.2 and 1.5. It also requires a support span/load span ratio (*L/t*) between 4 and 5 [35-16].

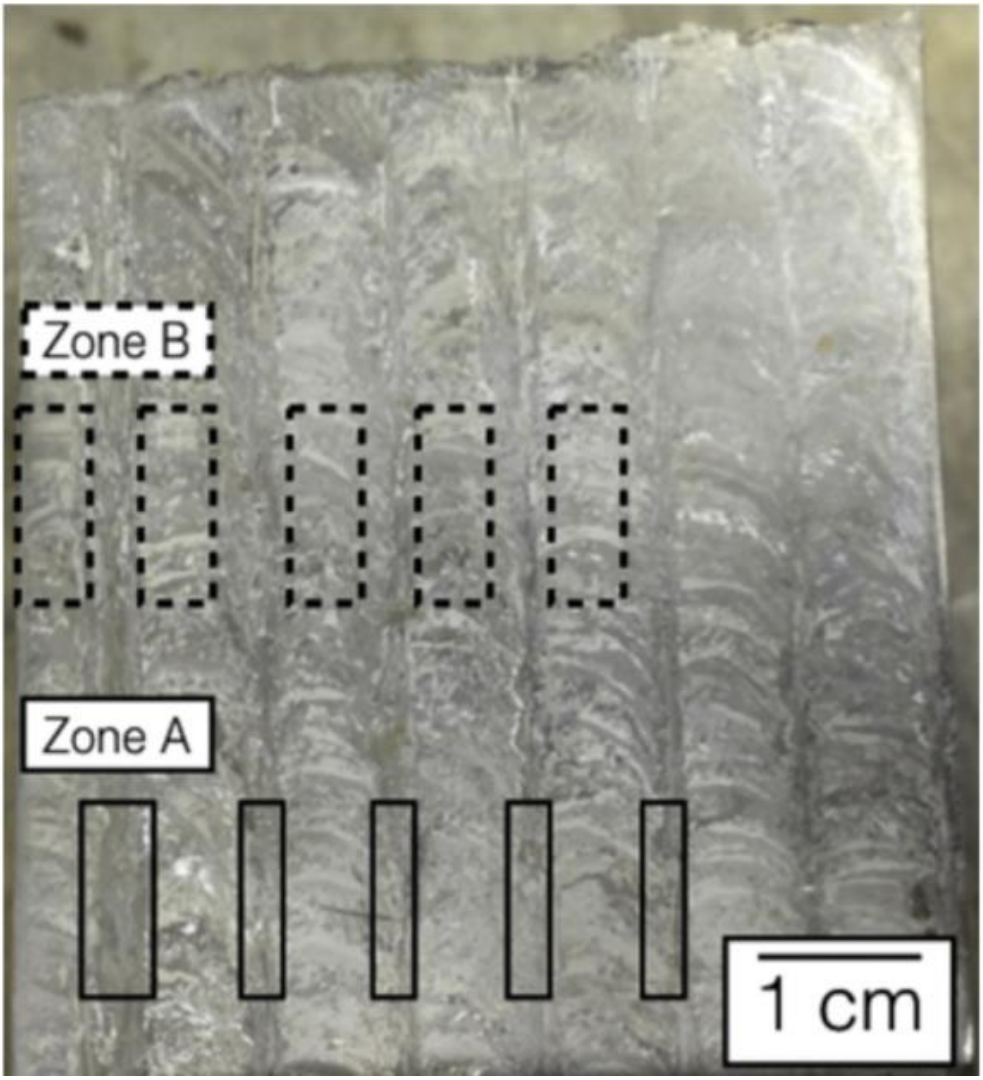


Fig. 4 Z-Y Cross-section of an ELI Ti-6Al-4V build [35-15].

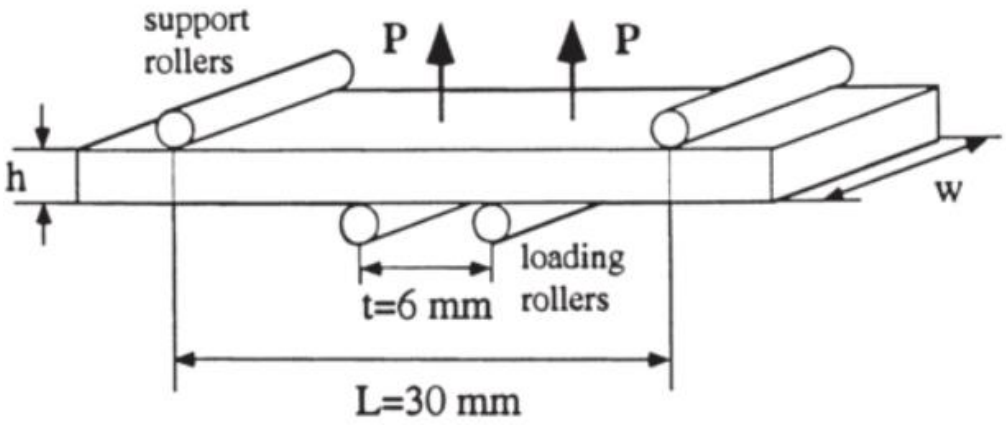


Fig. 5 Four-point bend specimen geometry and the loading states [35-16]

Conventional fatigue approach provides useful information of mechanical properties. However, several applications of Ti-alloys (e.g. Ti-6Al-4V) are required to safe operation over long periods of time, extending $10^9$ cycles [35-17]. Conventional fatigue tests as electromagnetic shakers or servo-hydraulic systems can achieve $10^9$ cycles in weeks, so a single S-N curve would last months [35-18]. This approach is impractical to understand the material behavior in this regime. Therefore, ultrasonic fatigue testing offers an alternative where $10^9$ cycles can be reached in less than a day. An ultrasonic fatigue system contains a generator, transducers (piezoelectric elements that generate the mechanical movement), booster, acoustic horn (typically acting as amplifier) and specimen (Fig. 6). Each part of the system has to satisfy the resonance condition [35-19]. This design is made in a way where the specimen has specific dimensions to offer a mode shape with maximum amplitude deformation on the specimen and not on any other part of the system [35-19, 35-20, 35-21]. Usually 20 KHz ± 500 Hz is the Eigenfrequency used to perform fatigue tests, a more detailed ultrasonic fatigue testing description can be found in [35-18, 35-19, 35-20, 35-22, 35-23]. Our approach here is again to evaluate a selective microstructure of an EBAM-Ti-6Al-4V process as for the conventional fatigue case ($10^7$ cycles), but in the regime of very high cycles ($10^9$). For this purpose, we will use an ultrasonic welding machine manufactured by Branson Ultrasonics with certain modifications to perform the fatigue test. The pre-selection of booster, horn, specimen shape and dimensions will be based on simulations of the process by COMSOL Multiphysics. A more detailed description of the general steps for the simulation can be found in [35-24].

In this study, we have three general objectives. First, we will assess tensile mechanical properties of the individual LFW zones as WZ, TMAZ and PM. Second, we will evaluate conventional fatigue mechanical properties of two zones (microstructures) of an EBAM-Ti-6Al-4V process. Finally, we will extend the analysis of the fatigue mechanical properties of the EBAM-Ti-6Al-4V process under the very high cycle regime. Additionally, we will adapt an ultrasonic welding machine into an ultrasonic fatigue machine.

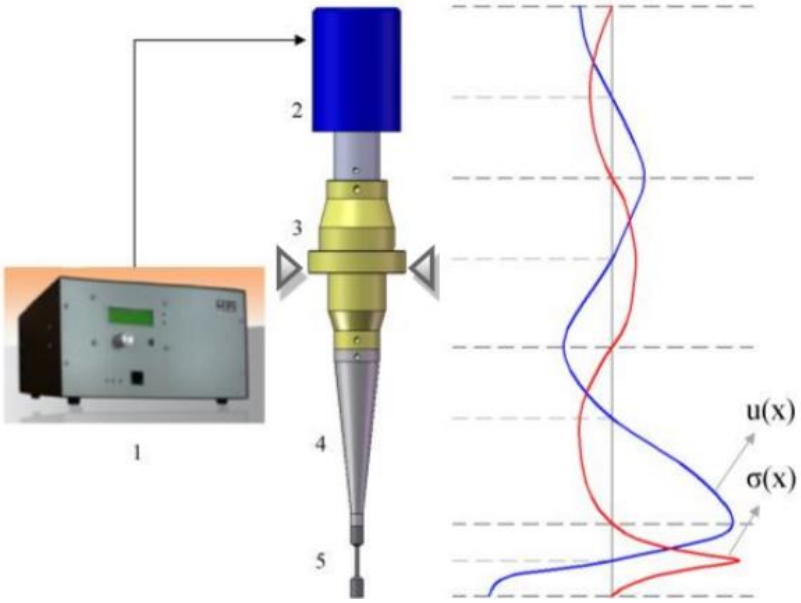


Fig. 6 Ultrasonic fatigue testing machine. 1-generator, 2- transducer, 3-booster, 4-horn, 5-specimen. u(x) displacement, □(x) stress [35-24]

### 35.3 Technical Plan and Recent Progress

More dogbone shape samples were extracted via EDM (Electron Discharge Machining) according to the availability of LFW-Ti-6AL-4V material to improve the statistics of the three zones of the process (Fig. 7). A ZwickLine Z2.5TN with screw grips type 8253 was used again for the tensile test of the three LFW zones and the TestXpert II software registered the respective Stress/Strain data and curves (Fig. 8).

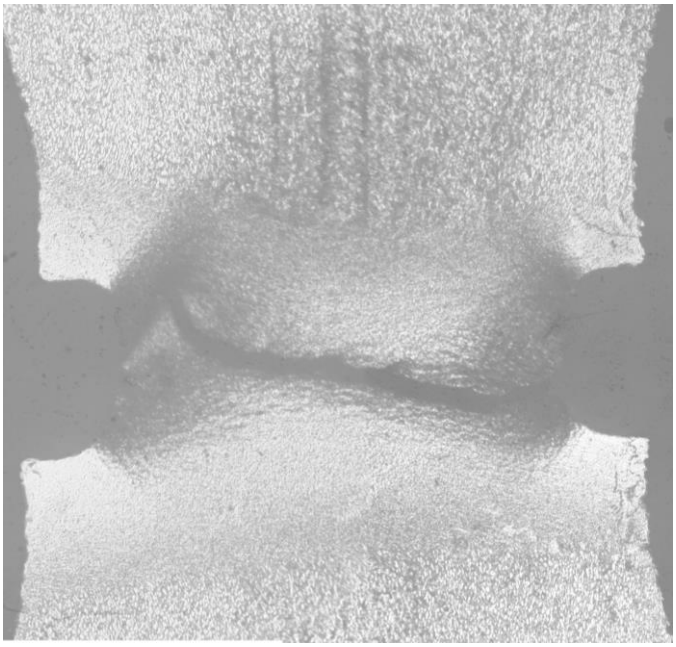

Fig. 7 WZ Tensile test specimens after test.

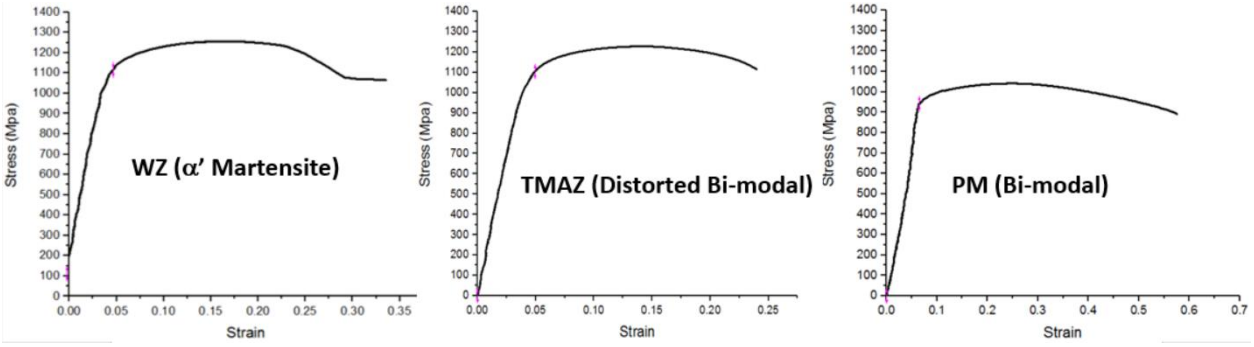


Fig. 8 Stress/ Strain curves for the three LFW-Ti-6Al-4V zones.

From this additional data, we can see that the yield strength is ~16% for the TMAZ and ~20% for the WZ greater than the PM zone. We know from similar tensile tests on LENS-Ti-6Al-4V that the yield stress is between 1 and 10% greater than the PM zone due to the martensitic microstructure. This difference suggests that another hardening mechanism is taking place.

Table. 1 Tensile properties of LFW-Ti-6AL-4V zones.

| | $Y_{0.2\%}$ (Mpa) | $U_{TS}$ (Mpa) | $R_{S}$ (Mpa) | %El | $Y_{HV}$ (Mpa) |
|---|---|---|---|---|---|
| WZ | 1175 | 1259 | 1106 | 24.7 | 1324 |
| TMAZ | 1141 | 1245 | 1068 | 31.0 | 1196 |
| PM | 976 | 1040 | 886 | 56.4 | 1098 |

In order to understand if strain hardening is taking place, PED-TEM analysis has been performed on the LFW zones to evaluate the dislocation density (Fig. 9). The Euler orientation information from PED is the input file for a MATLAB developed code [35-25] to calculate the dislocation density. Knowing from literature that the modulus of elasticity E of $\alpha$ titanium single crystal is inversely proportional of angle $\gamma$ between the c-axis of the unit cell and the stress axis, polycrystalline $\alpha$ titanium with texture has to be considered. For this purpose, EBSD maps of all three zones will be useful to evaluate the influence of texture on the tensile mechanical properties (Fig. 10).

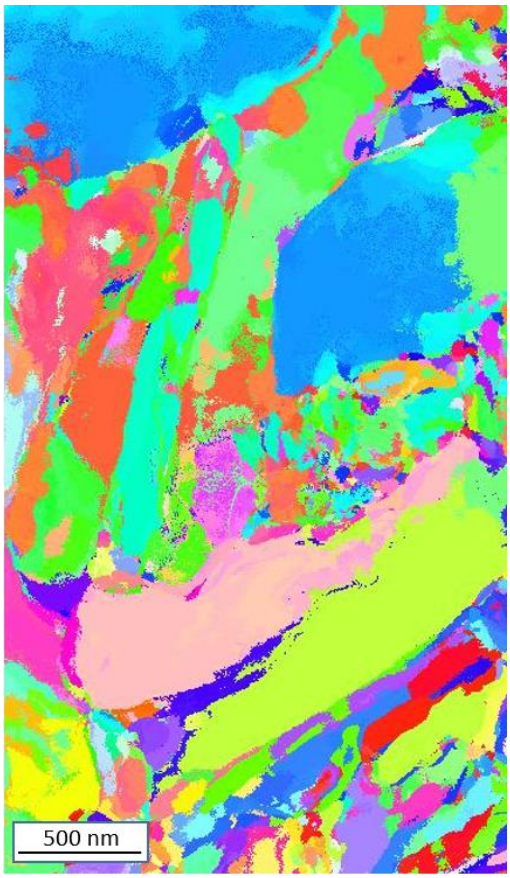


Fig. 9 PED-TEM orientation data of WZ for dislocation density analysis

The EBSD maps reveal that the orientation is random as a consequence of LFW. From these results, texture can be discarded as a factor of influence to the tensile properties and more specifically to the yield strength. However, the randomness of orientation in the WZ suggests high values of pressure during the LFW process based on the results of Romero et al. [35-2]. On the other hand, the randomness in orientation in the TMAZ is corresponding with the specimen scale size of Karadge et al. [35-4], but still with no clear explanation of the reason.

More effort has been taking place to perform the dislocation density calculation and data from EBSD maps such as zero solution fraction (i.e. unindexed fraction), aspect ratio of primary $\alpha_p$ grains as a consequence of TMAZ deformation and other features from MIPAR analysis of SEM-EBSD images of the LFW zones.

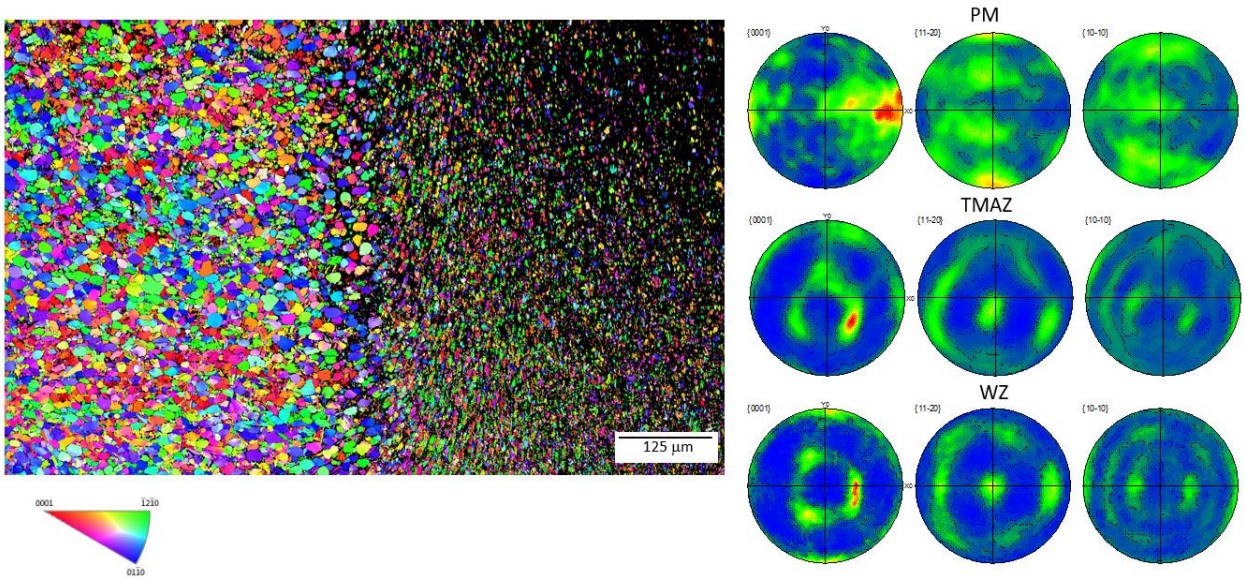


Fig. 10 IPF-Z EBSD map and pole figures showing the random orientation of LFW zones

To assess the conventional fatigue mechanical properties of zones A and B (i.e. microstructures of EBAM-Ti-6Al-4V) a four-point bending test will be performed. 20 specimens total, 10 for zone A and 10 for zone B were sectioned via EDM with the suitable dimensions for capturing the interested microstructure (Fig. 11). The specimens were chamfered on sharp edges and polished on surfaces to be tested at Westmoreland Mechanical Testing and Research, Inc. The S-N curve and fracture mechanics will be evaluated on those two microstructures.


Fig. 11 Conventional fatigue beams sectioned via EDM, chamfered, polished and etched.

Ultrasonic fatigue test demands an extra effort on this study. First, the ultrasonic system is modeled with COMSOL Multiphysics to see its response by trial and error changing the acoustic horn, shape and dimensions of the test specimen. All the information of the ultrasonic system is provided by Branson Ultrasonics (Fig. 12). The response should match with an estimated lower stress on specimen of 460 Mpa and a higher stress of 980 Mpa (common limit values for a regular S-N curve of Ti-6Al-4V). The sequence of this modeling is first to determine the Eigenfrequency around 20 kHz with the desired mode shape on cantilevers. Once the eigenfrequency is determined a frequency domain study is done to determine the input power values for the system to show the stress levels required to match. The cantilever specimens with the calculated dimensions were sectioned via EDM, polished and etched. The Zones A and B of the EBAM-Ti-6Al-4V material are clearly visible on the etched specimen in Fig. 13. However the thickness reduction required by the model on the cantilevers can not be performed by EDM, then a special mini Grinder/polisher similar to a GATAN Dimpler was designed and built for this purpose. The predicted eigenfrequency and the

correlation of the stress levels with the amplitude displacements from COMSOL Multiphysics will be corroborated with the experimental data from the Branson ultrasonic equipment. We assume a successful prediction and a close performance of the test to construct the S-N curve in the regime of $10^9$ cycles to assess the fracture mechanics.

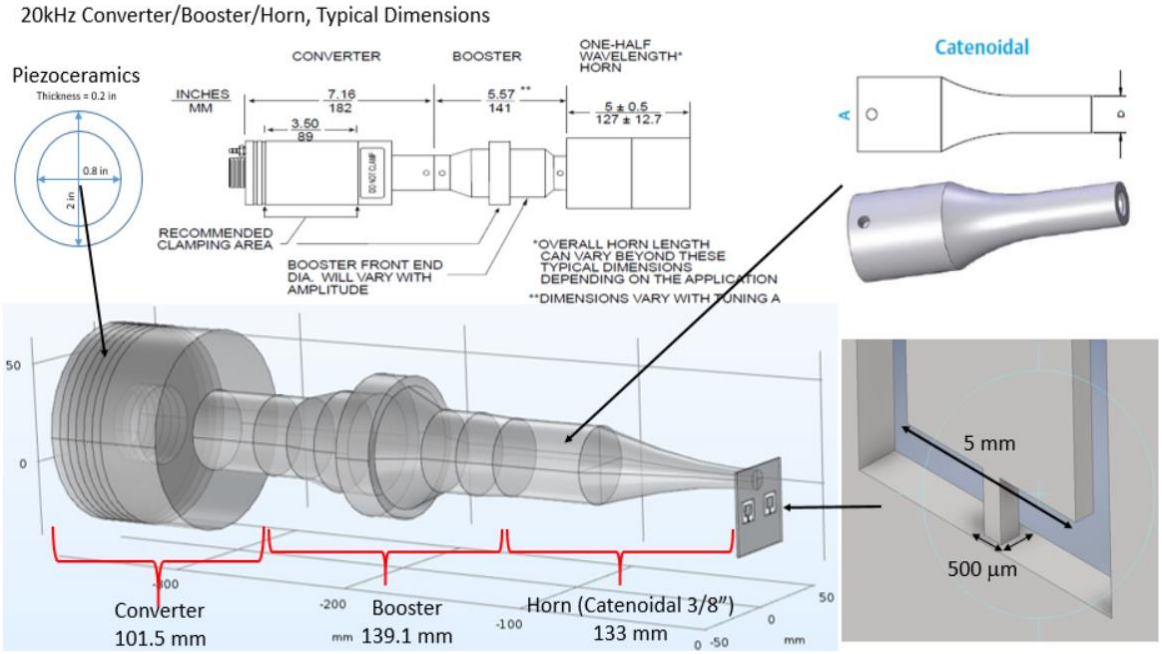


Fig. 12 Comsol model of the ultrasonic fatigue system according to Branson Ultrasonic equipment.

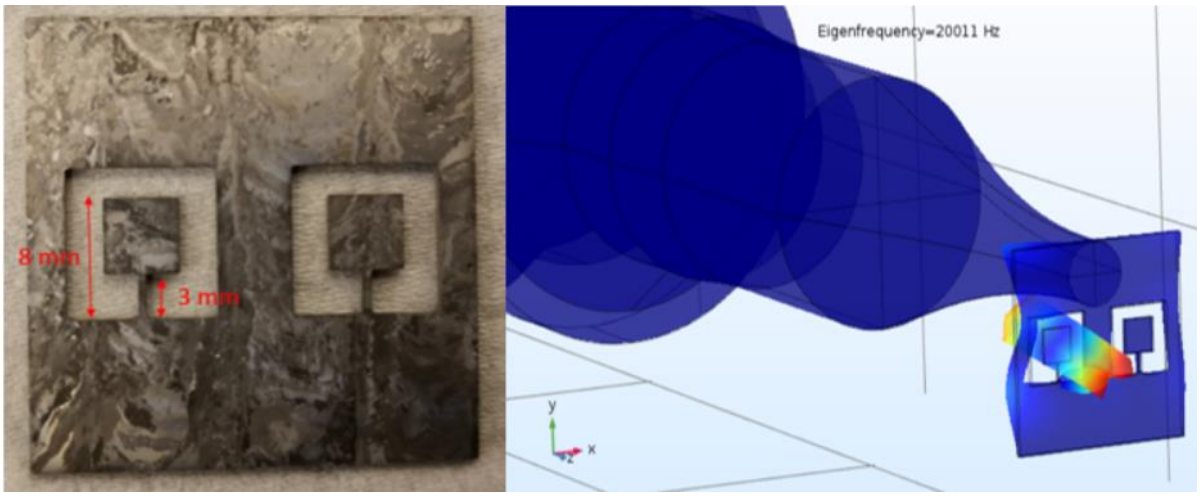


Fig. 13 Cantilever sectioned via EDM with the calculated dimension, and the mode shape of cantilever vibration.

### 35.4 Expected Results

We believe that the mechanism that is acting is strain hardening, from this perspective dislocation density measurements are necessary to differentiate the LFW zones and the LENS-Ti-6Al-4V microstructures. On the four-point bending fatigue experiment, we know that the zone B has a bigger variation in α' lath thickness and orientation. We expect that crack propagation in zone B would be lower than in zone A. This is under the argument that in very fine lamellar microstructures with individual α' laths more randomly oriented in zone B than A, a crack would have more deviated slip systems (stronger obstacles) on those adjacent α' laths to overcome. Therefore, if there is a

difference in the S-N curves for those microstructures would be in that direction. Westmoreland Mechanical Testing and Research Inc. will provide results on this test in the coming weeks.

The ultrasonic fatigue test offers even more challenges. COMSOL Multiphysics model predicted the shape and dimensions of the samples to show a suitable mode shape of bending for the cantilevers for the fatigue test. Even when the first test on Branson was a failure due to complete destruction of the specimen (See Fig. 14), the second test with a more controlled power was successful in terms of the cantilever oscillation and guided failure of the cantilever as designed (see Fig. 15). The expectation respect to the S-N curves and fracture analysis are about the same as for the conventional fatigue analysis (four-point bend test), but with the uncertainty of the different strain rate and very high frequency influence on the test. The current work is focus into installation and set-up of the UT-Branson equipment and more specimen's preparation.

Our objectives in terms of publications are at least two. First, tensile properties on individual LFW zones have not been studied in detail to date. Second, EBAM-Ti-6AL-4V process has been studied before and tensile properties have been reported in the past, but fatigue analysis have not been performed on those individual microstructures to date. Additionally, even when ultrasonic fatigue test is not new, there is just a few studies on it and no one specifically on EBAM-Ti-6Al-4V cantilevers.

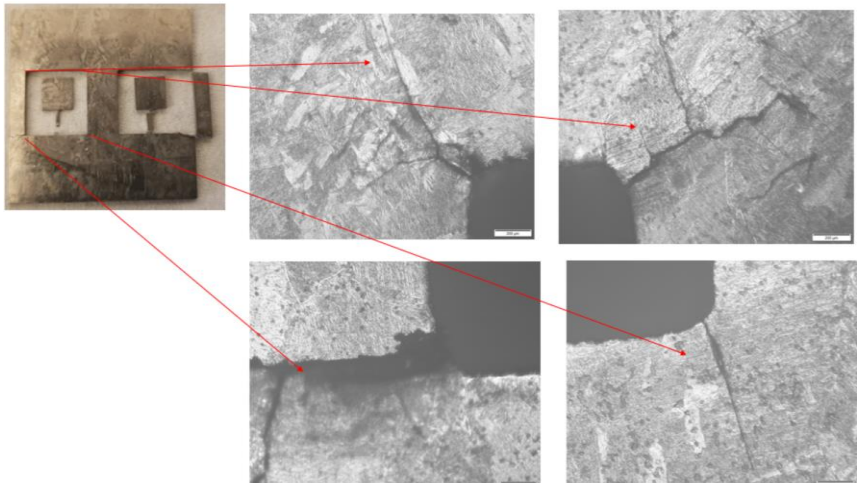

Fig. 14 First ultrasonic fatigue test on the Branson equipment (Failure)

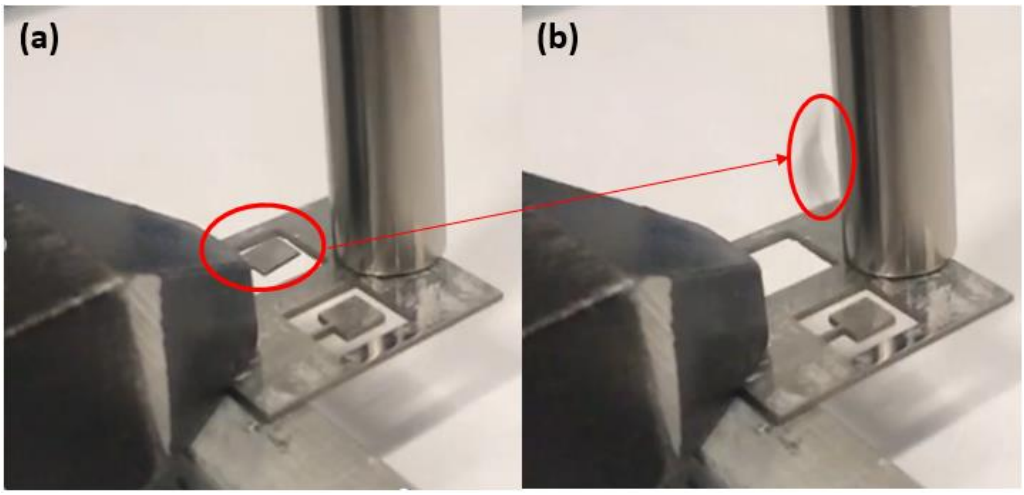


Fig. 15 Second ultrasonic fatigue test on the Branson equipment (a) before and (b) after (successful)

## 35.5 References


[35-1] P. Wanjara, M. Jahazi, Linear friction welding of Ti-6Al-4V: Processing, microstructure, and mechanical-property inter-relationships, Metallurgical and Materials Transactions A 36(8) (2005) 2149-2164.
[35-2] J. Romero, M.M. Attallah, M. Preuss, M. Karadge, S.E. Bray, Effect of the forging pressure on the microstructure and residual stress development in Ti–6Al–4V linear friction welds, Acta Materialia 57(18) (2009) 5582-5592.
[35-3] I. Bhamji, M. Preuss, P.L. Threadgill, A.C. Addison, Solid state joining of metals by linear friction welding: a literature review, Materials Science and Technology 27(1) (2011) 2-12.
[35-4] M. Karadge, M. Preuss, C. Lovell, P.J. Withers, S. Bray, Texture development in Ti–6Al–4V linear friction welds, Materials Science and Engineering: A 459(1-2) (2007) 182-191.
[35-5] Y. Guo, Y. Chiu, M.M. Attallah, H. Li, S. Bray, P. Bowen, Characterization of dissimilar linear friction welds of α-β titanium alloys, Journal of materials engineering and performance 21(5) (2012) 770-776.
[35-6] A.R. McAndrew, P.A. Colegrove, C. Bühr, B.C.D. Flipo, A. Vairis, A literature review of Ti-6Al-4V linear friction welding, Progress in Materials Science 92 (2018) 225-257.
[35-7] A. Vairis, M. Frost, High frequency linear friction welding of a titanium alloy, Wear 217(1) (1998) 117-131.
[35-8] A. Vairis, M. Frost, On the extrusion stage of linear friction welding of Ti 6Al 4V, Materials Science and Engineering: A 271(1-2) (1999) 477-484.
[35-9] A.R. McAndrew, P.A. Colegrove, A.C. Addison, B.C.D. Flipo, M.J. Russell, Energy and Force Analysis of Ti-6Al-4V Linear Friction Welds for Computational Modeling Input and Validation Data, Metallurgical and Materials Transactions A 45(13) (2014) 6118-6128.
[35-10] W.Y. Li, T. Ma, Y. Zhang, Q. Xu, J. Li, S. Yang, H. Liao, Microstructure Characterization and Mechanical Properties of Linear Friction Welded Ti-6Al-4V Alloy, Advanced Engineering Materials 10(1-2) (2008) 89-92.
[35-11] W. Li, H. Wu, T. Ma, C. Yang, Z. Chen, Influence of Parent Metal Microstructure and Post-Weld Heat Treatment on Microstructure and Mechanical Properties of Linear Friction Welded Ti-6Al-4V Joint, Advanced Engineering Materials 14(5) (2012) 312-318.
[35-12] K. Hiroshi, N. Koji, T. Wakabayashi, N. Kenji, Application of linear friction welding technique to aircraft engine parts, IHI Engineering Review 47(1) (2014) 40-43.
[35-13] P.C. Collins, D.A. Brice, P. Samimi, I. Ghamarian, H.L. Fraser, Microstructural Control of Additively Manufactured Metallic Materials, Annu. Rev. Mater. Res. 46(1) (2016) 63-91.
[35-14] Sciaky, Sciaky's Electron Beam Additive Manufacturing (EBAM®) Process. <http://www.sciaky.com/additive-manufacturing/wire-am-vs-powder-am>, 2019).
[35-15] B.J. Hayes, B.W. Martin, B. Welk, S.J. Kuhr, T.K. Ales, D.A. Brice, I. Ghamarian, A.H. Baker, C.V. Haden, D.G. Harlow, H.L. Fraser, P.C. Collins, Predicting tensile properties of Ti-6Al-4V produced via directed energy deposition, Acta Materialia 133 (2017) 120-133.
[35-16] T. Zhai, Y. Xu, J. Martin, A. Wilkinson, G. Briggs, A self-aligning four-point bend testing rig and sample geometry effect in four-point bend fatigue, International Journal of Fatigue 21(9) (1999) 889-894.
[35-17] M. Janeček, F. Nový, P. Harcuba, J. Stráský, L. Trško, M. Mhaede, L. Wagner, The Very High Cycle Fatigue Behaviour of Ti-6Al-4V Alloy, Acta Physica Polonica, A. 128(4) (2015).
[35-18] R. Morrissey, P.J. Golden, Ultrasonic fatigue testing of Ti-6Al-4V, Journal of ASTM International 2(5) (2005) 1-10.
[35-19] A. Puškár, Ultrasonic fatigue testing equipment and new procedures for complex material evaluation, Ultrasonics 31(1) (1993) 61-67.
[35-20] A. Puskar, The use of high-intensity ultrasonics, Amsterdam, Elsevier Scientific Publishing Co.(Materials Science Monographs. Volume 13), 1982. 302 p. Translation, 1982.
[35-21] J. Gong, A. Wilkinson, Ultra small scale high cycle fatigue testing by micro-cantilevers, Nanomechanical Testing in Materials Research and Development V, Grande Real Santa Eulalia Hotel, Albufeira, Portugal, 2015.
[35-22] M. Freitas, V. Anes, D. Montalvao, L. Reis, A. Ribeiro, Design and assembly of an ultrasonic fatigue testing machine, Anales de Mecânica de la Fractura (2011).
[35-23] A. Shyam, C. Torbet, S. Jha, J. Larsen, M. Caton, C. Szczepanski, T. Pollock, J. Jones, Development of ultrasonic fatigue for rapid, high temperature fatigue studies in turbine engine materials, 10th International Symposium on Superalloys, Champion, PA, September, 2004, pp. 19-23.
[35-24] D.M. Dimitrov, V. Mihailov, B. Kostov, Modeling of Ultrasonic Fatigue-Life Testing Machine, Proceedings of COMSOL conference, Milan, 2012.

[35-25] I. Ghamarian, Application of ASTAR/precession electron diffraction technique to quantitatively study defects in nanocrystalline metallic materials, (2017).